Appeared In Complex Light and Optical Forces, eds. D.L. Andrews, E. J. Galvez, G. Nienhuis, Vol. 6483, p. 64830I SPIE, 2007

Complex beam sculpting with tunable acoustic gradient index lenses

Euan McLeod and Craig B. Arnold

Department of Mechanical & Aerospace Engineering, Princeton University, Princeton, NJ

ABSTRACT

Spatial Light Modulators (SLMs) have been successfully used for beam sculpting in the area of optical manipulation, however in some applications their associated pixelation, slow switching speeds, and incident power limitations can be undesirable. An alternative device that overcomes these problems is the Tunable Acoustic Gradient index (TAG) lens. This device uses acoustically induced density and refractive index variations within a fluid to spatially phase modulate a transmitted laser beam. The acoustic waves within the fluid are generated via a piezoelectric transducer. When driven with a frequency-modulated signal, arbitrary optical phase modulation patterns can be generated at regular time intervals. The resulting sculpted beam is best observed using a pulsed laser synchronized to the frequency-modulated signal of the TAG lens. As this device is purely analog, there is no pixelation in the phase modulation pattern. Also, because the only major requirement on the fluid is that it be transparent, it is possible to select fluids with high damage thresholds and high viscosities. High damage thresholds allow the TAG lens to be used in high power applications that would be unsuitable for an SLM. High viscosities provide fast damping of transient density variations and increase switching speeds between patterns. Discussion here will be limited to axially symmetric beam sculpting, however the results can be generalized to asymmetric cases.

Keywords: TAG Lens, Beam Sculpting, Acoustics, Phase Modulation

1. INTRODUCTION

Laser beam shaping has lately become of interest especially in the fields of optical manipulation and atom optics. In optical micromanipulation alone, the resulting complex beams have been used in many applications. A few examples include particle sorting and cytometry,[1,2] microfluidic pumps,[3] the study of 2D colloidal phase transformations,[4,5] and the assembly of of microscopic structures.[6] In atom optics, uses for complex beams include trapping atoms in an optical bottle beam[7] and transporting cold atoms.[8]

Currently, the demand for adaptive optics in the fields of optical manipulation and atom optics has been met primarily using using spatial light modulators (SLMs).[9,10] However, SLMs do have some limitations. First, they are digital devices, and as a result their output is pixellated, which can degrade beam quality. Second, they have limited refresh rates. Typical spatial light modulators use nematic liquid crystal arrays. Reorienting the liquid crystals is a relatively slow process that limits frame rates to around 100Hz.[11] There do exist ferroelectric SLMs that can operate at rates above 1kHz, however these devices are only binary spatial light modulators; that is, each pixel can only impart one of two given phase delays on the wavefront.[11] Third, SLMs have incident laser power limitations due do the delicate nature of the liquid crystals.

An alternative method for adaptive optics is the liquid-filled tunable acoustic gradient index (TAG) lens.[12–14] This method can be thought of as an analog counterpart to the currently digital adaptive optics. TAG lenses do not have the same limitations as SLMs, and therefore may be more suitable in some applications. First, TAG lenses are analog, so there are no pixellation effects. Second, they have fast switching speeds, as high as 20 kHz, although for optimum pattern quality, refresh rates closer to 1 kHz were used.[13] Switching speed can be improved by filling the TAG lens with fluids having a greater viscosity and speed of sound. Third, because a wide range of filling fluids are available, it is possible to design the TAG lens to withstand very large laser powers.

Further author information: E-mail: emcleod@princeton.edu

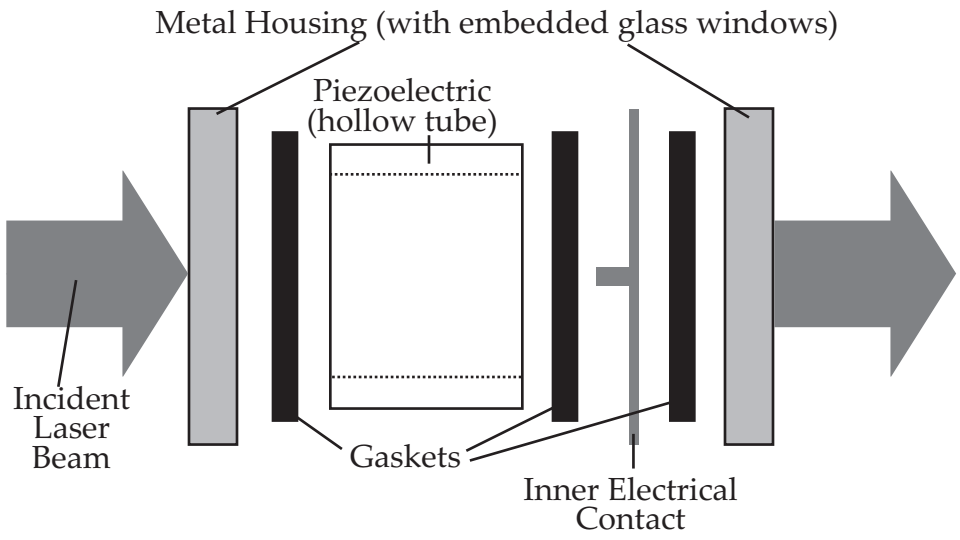

Figure 1. Cartoon illustrating the construction of the TAG lens.

This proceeding will demonstrate that TAG lenses have the potential to be significantly more versatile than has been previously reported. So far, these lenses have been shown only to produce multiscale Bessel beams using single-frequency input signals.[12,14] By using more complicated, multiple frequency signals, it is possible to generate approximations to arbitrary spatial refractive index distributions throughout the lens. Currently, only axisymmetric TAG lenses have been studied, however the ideas presented in this proceeding can be extended to rectangular geometries, allowing a wider range of allowable beam shapes.

2. TAG LENS BASICS

The full description of the TAG lens has been provided in other publications,[12–14] however a quick overview of the device follows. The lens operates by generating acoustic variations in density within a fluid. These density variations create a gradient in refractive index, allowing the device to function as an optical lens. Previous TAG lenses have come in the form of a cylindrical cavity filled with a transparent liquid. The assembly of such a TAG lens is illustrated in Fig. 1. The circumference of the chamber is a hollow piezoelectric tube, which is electrically driven in the radial direction to generate acoustic waves that propagate toward the center of the chamber. In steady state, single frequency operation, this device has been shown to produce multiscale Bessel beams.[12]

3. PROCEDURE

3.1. Frequency Response

The end goal of the following procedures is to solve the *inverse problem*: determining what voltage signal is necessary to generate a desired refractive index profile. However, before directly tackling this question, it is easier first to find the response of the lens to a single frequency, and then to solve the *forward problem* addressed in the next section: determining the index profile generated by a given voltage input.

The first step of the procedure is to find the frequency response of the TAG lens. We assume a linear model of the TAG lens.[14] That is, the oscillating refractive index created within the lens is linear with respect to the driving frequency. Listed below are the single-frequency input signal and resulting output refractive index within the lens.

$$V(t,f) = \mathrm{Re}\left[\hat{V}(f)\, e^{2\pi i f t}\right] \quad (1)$$

$$n(r,t,f) = n_0 + \mathrm{Re}\left[\hat{n}(f)\, J_0(2\pi k r)\, e^{2\pi i f t}\right]. \quad (2)$$

Here, f is the electrical driving frequency of the lens, n_0 is the static refractive index of the lens, $\hat{V}(f)$ is the driving voltage complex amplitude, and k is the spatial frequency given by f/c_s where c_s is the speed of sound within the fluid.

From this frequency response, a transfer function can be defined to relate the index response to the voltage input:

$$\Phi(f) \equiv \frac{\hat{n}(f)}{\hat{V}(f)} \in \mathbb{C}. \tag{3}$$

This transfer function can either be determined empirically, or through modelling,[14] and accounts for both variations in amplitude and phase.

3.2. Forward Problem

For the forward problem, we assume that the lens is driven with a discrete set of frequencies at varying amplitudes and phase shifts. One could also phrase the problem in terms of a continuous set of input frequencies, however as is seen later, the solution to the discrete set will be more useful when dealing with the inverse problem.

We assume an input signal of the form,

$$V(t) = \mathrm{Re}\left[\sum_{m=1}^{M} \hat{V}_m e^{2\pi i f_m t}\right], \tag{4}$$

where each $\hat{V}_m$ is a given complex amplitude.

By linearity and the results of the frequency response in Eq. 2, the corresponding refractive index in the lens is known to be,

$$n(r,t) = n_0 + \mathrm{Re}\left[\sum_{m=1}^{M} \hat{n}_m \, J_0(2\pi k_m r) \, e^{2\pi i f_m t}\right]. \tag{5}$$

The coefficients $\hat{n}_m$ can be determined from the frequency response to be,

$$\hat{n}_m = \Phi(f_m)\hat{V}_m. \tag{6}$$

Eqs. 5 and 6 are the solution to the forward problem.

3.3. Inverse Problem

The inverse problem is to determine what input voltage signal, $V(t)$, is required to produce a desired refractive index profile, $n_{goal}(r)$. From Eqs. 1 and 2, it is evident that the actual refractive index is a function of both space and time, while the input electrical driving signal is only a function of time. As a result, it is not possible to create any arbitrary index of refraction profile defined in both space and time, however this paper will show that it is possible to approximate an arbitrary spatial profile that repeats periodically in time. We will assume that the arbitrary profile is centered around the static index of refraction, n_0. We will denote the deviation of the goal from n_0 as $n_{goal}(r)$, and the frequency with which it repeats in time as f_{rep}.

The procedure is depicted as a flow chart in Fig. 2. First, $n_{goal}(r)$ is decomposed into its spatial frequencies using a Fourier-Bessel transform. This result is then discretized so that only spatial frequencies that are integer multiples of f_{rep}/c_s are included. Then, in order to write the index response in the form of Eq. 5, an inverse Fourier-Bessel transform is applied to the discrete series. This gives the coefficients $\hat{n}_m$, which are used in conjunction with the frequency response to yield the required voltage signal in the frequency domain. Summing over all modes provides the final answer, $V(t)$.

The first step is to decompose the desired index profile into its spatial frequencies using a windowed Fourier-Bessel transform because of the circular geometry of the lens. Given $n_{goal}(r)$, $\hat{n}_{goal}(k)$ can be computed as,

$$\hat{n}_{goal}(k) = \int_0^{r_0} n_{goal}(r) \, J_0(2\pi r k) \, 2\pi r \, dr, \tag{7}$$

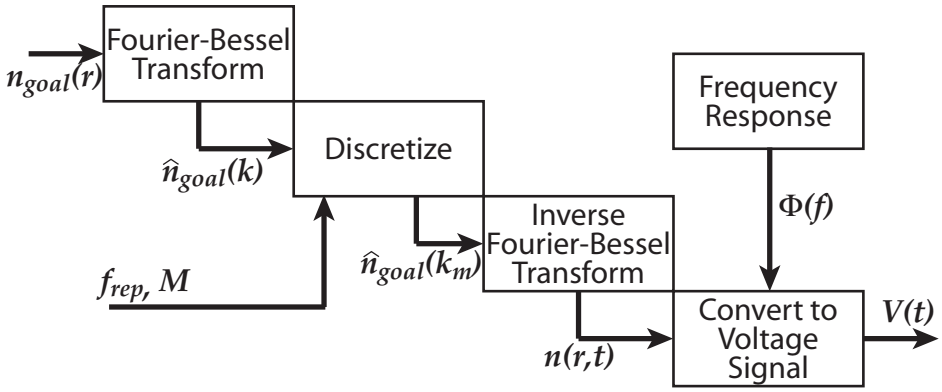

Figure 2. Flow chart of process for solving the inverse problem.

where r_0 is the inner radius of the lens. Depending on the desired index goal, $n_{goal}(r)$, this windowing may introduce undesirable Gibbs phenomenon effects near the edge of the lens if $n_{goal}(r)$ does not smoothly transition to zero at $r = r_0$. However, the significance of these effects can be reduced by either modifying the goal signal, extending the limit of integration beyond r_0, or simply using an optical aperture to obscure the outer region of the lens.

From inverse-transforming we know that,

$$n_{goal}(r) = \int_0^\infty \hat{n}_{goal}(k)\, J_0(2\pi k r)\, 2\pi k\, dk. \tag{8}$$

However, each of the spatial frequencies will oscillate in time at its own frequency given by $f = c_s k$. As a result, the goal pattern can only generated at one point in time. If this time is $t = 0$, then the time dependent index of refraction will be given by,

$$n_{goal}(r,t) = \mathrm{Re}\left[\int_0^\infty \hat{n}_{goal}(k)\, J_0(2\pi k r)\, 2\pi k\, e^{2\pi i f(k) t}\, dk\right] \tag{9}$$

In practice, one would wish the goal index pattern to repeat periodically in time, as opposed to achieving it only at one instant in time. Therefore, the second step of the procedure is to discretize the spatial frequencies used so that the $n_{goal}(r)$ can be guaranteed to repeat with temporal frequency f_{rep}. This is acheived by only selecting spatial frequencies that are multiples of f_{rep}/c_s. That is, we assume that,

$$k \in \{k_m\}_{m=1}^{M} = \left\{ m \frac{f_{rep}}{c_s} \right\}_{m=1}^{M}. \tag{10}$$

The upper limit, M, is set sufficiently large so that the contribution to $n_{goal}(r)$ is negligible from spatial frequencies higher than $M f_{rep}/c_s$. It is also required that $n_{goal}(r)$ and f_{rep} are chosen so that the contribution is negligible from spatial frequencies lower than f_{rep}/c_s and so that the discretization accurately approximates the continuous function. The lower f_{rep}, the more accurately the discretization will reflect the continuous solution, however it also means that there will be longer intervals between pattern repetition.

This discretization changes the integral in Eq. 9 into a sum:

$$n(r,t) = n_0 + \mathrm{Re}\left[\sum_{m=1}^{M} \hat{n}_{goal}(k_m)\, J_0(2\pi k_m r)\, 2\pi k_m\, e^{2\pi i f_m t}\, \Delta k\right], \tag{11}$$

where Δk is the spacing between spatial frequencies, in this case given by f_{rep}/c_s. The third step of the procedure is to compute this sum. At this point, one should compare $n_{goal}(r)$ with $n(r,0)$ to ensure good agreement. If the

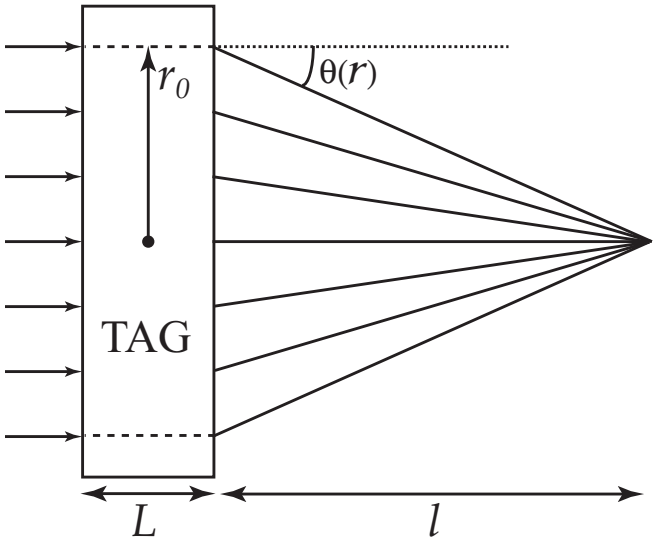

Figure 3. Figure illustrating a TAG lens acting as a simple converging lens.

agreement is poor, lowering f_{rep}, raising M, smoothing $n_{goal}(r)$, and continuing the integration in Eq. 7 beyond r_0 can all improve the approximation.

By comparing Eq. 11 with Eq. 5 from Section 3.2, it is evident that,

$$\hat{n}_m = 2\pi k_m \, \Delta k \, \hat{n}_{goal}(k_m). \tag{12}$$

Using the frequency response in Eq. 6 and rewriting k_m and Δk in terms of f_{rep}, this expression can be used to find the voltage signal coefficients:

$$\hat{V}_m = \frac{2\pi m \, f_{rep}^2 \, \hat{n}_{goal}(k_m)}{c_s^2 \Phi(f_m)}. \tag{13}$$

The time domain signal is given by the same expression as in Section 3.2,

$$V(t) = \mathrm{Re}\left[\sum_{m=1}^{M} \hat{V}_m \, e^{2\pi i f_m t}\right]. \tag{14}$$

Eqs. 13 and 14 represent the last step and solution to the inverse problem.

4. EXAMPLE

In this section, we present an example problem, where we wish to create a simple converging lens with a specific focal length, l, as shown in Fig. 3. Given this criteria, we wish to determine the voltage signal to be supplied to the TAG lens so that it adopts this converging lens configuration with temporal period t_{rep}. The parameters for the TAG lens in this example are given in Table 1. For the sake of simplicity in illustrating the above procedure, we will assume a constant frequency response, $\Phi(f)$. Note that in reality, $\Phi(f)$ would vary greatly with frequency near resonances within the lens. However, since this affects only the last step of the procedure, the exact form of the function, while important for practical implementation, is unimportant here in demonstrating the solution process. The form of $\Phi(f)$ is discussed in detail in a forthcoming paper.[14]

The first step of this example is to determine the refractive index profile for a simple converging lens with this focal length. Using small angle approximations, the angle by which normally incident incoming rays should be deflected is given by,

$$\theta_{goal}(r) = -r/l. \tag{15}$$

Table 1. Parameters used in the example inverse problem.

Name	Symbol	Value
Focal Length	l	1 m
Temporal Period	t_{rep}	1 ms
Inner Radius	r_0	5 cm
Lens Length	L	5 cm
Sound Speed	c_s	1000 ms^{-1}
Transfer Func.	$\Phi(f)$	10^{-3} V^{-1}
Largest Mode	M	300

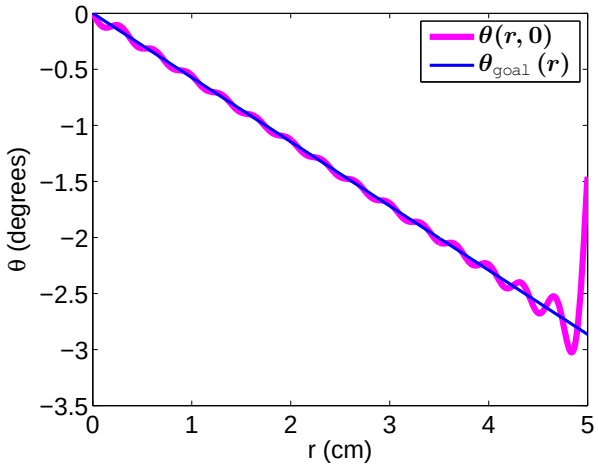

Figure 4. Figure showing both the goal and the actual deflection angle as a function of radius at time $t = 0$.

This goal angular deflection is shown in Fig. 4.

The corresponding refractive index profile required to deflect rays by this angle is given by,

$$n_{goal}(r) = \frac{1}{L}\int_0^r \theta_{goal}(r')dr' = -\frac{r^2}{2Ll}. \tag{16}$$

This function is plotted in Fig. 5.

The procedure described in Section 3.3 is now followed to obtain $V(t)$. Eq. 7 is used to decompose the goal refractive index into its spatial frequencies. These spatial frequencies are then discretized with the lower bound and spacing between frequencies given by $f_{rep} = 1/t_{rep} = 1\,\text{kHz}$. The upper bound is chosen to be 300 kHz, which corresponds to $M = 300$. Both the continuous and discretized spatial frequencies are plotted in Fig. 6. The value of M was chosen large enough so that the actual angular deflection reasonably approximates the goal, as shown in Fig. 4.

The actual index of refraction at time $t = 0$ is obtained from the discretized frequencies using Eq. 11 and is plotted in Fig. 5. Note the very good agreement between the goal and actual refractive index profiles. This good agreement is due to f_{rep} being relatively small, and M being relatively large.

The angular deflection is obtained by differentiating the refractive index profile. This deflection is plotted in Fig. 4. Note that the discrepancy between the goal and actual angular deflections is amplified relative to the refractive index profile. This is because of the amplifying properties of the derivative. However, there is still good agreement between the goal and actual deflections, except at the edge of the lens where the Gibbs phenomenon can be observed because the refractive index does not smoothly transition to zero there. Better agreement could

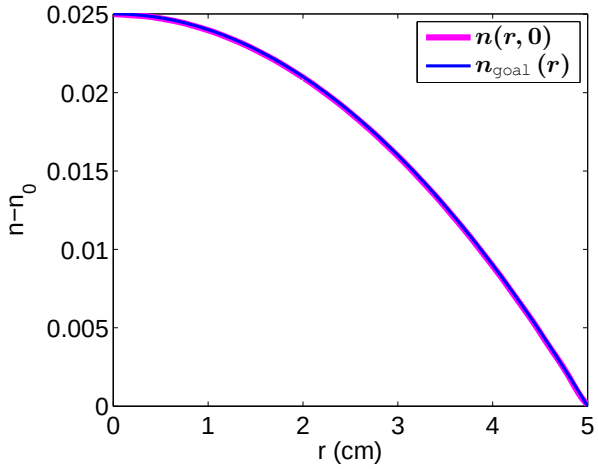

Figure 5. Figure showing both the goal and the actual refractive index as a function of radius at time $t = 0$.

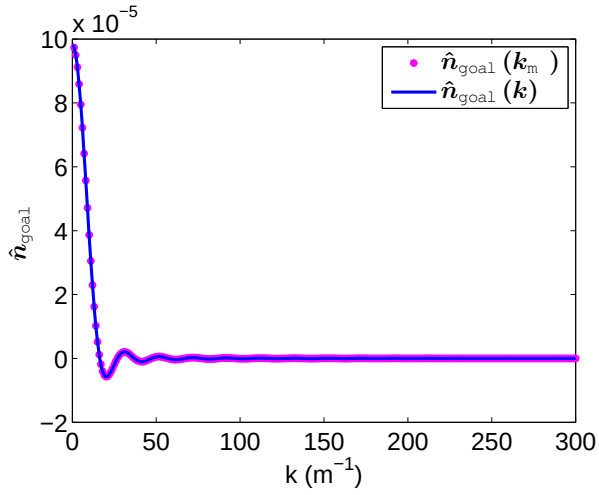

Figure 6. Figure showing both the continuous and discretized spatial frequencies of $n_{goal}(r)$.

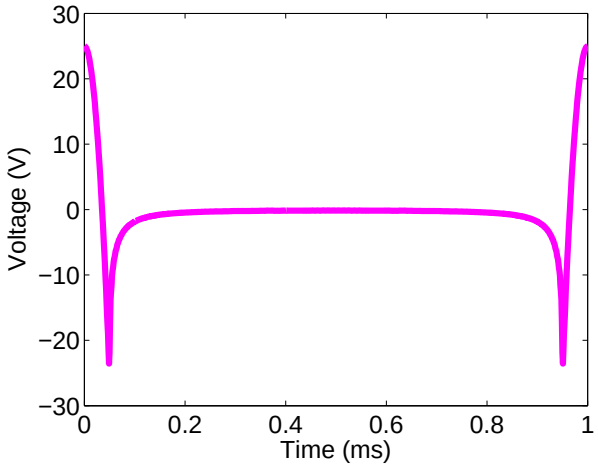

Figure 7. Figure showing one period of the time domain voltage signal required to generate the actual lensing effects portrayed in Figs. 4 and 5.

be achieved by choosing a larger M or smoothing out the desired index goal. In some situations, choosing a larger t_{rep} would also be helpful.

Using Eqs. 13 and 14, the actual voltage signal can be computed. It is periodic with period t_{rep}. One period is plotted in Fig. 7. It is important to note that changes in $\Phi(f)$ can change the form of this function. This signal can be input into a function generator to drive the lens.

5. CONCLUSIONS

A method has been presented to approximately generate arbitrary axisymmetric index patterns, which repeat at regular intervals. This allows a cylindrical TAG lens to act as an axisymmetric spatial light modulator. If instead of a cylindrical geometry, a rectangular geometry was used for the TAG lens with two orthogonal piezoelectric actuators, then arbitrary two dimensional patterns may be approximated without the axisymmetric limitation. The only mathematical difference will be the use of Fourier transforms instead of using Fourier-Bessel transforms to determine the spatial frequencies.

Compared to nematic liquid crystal SLMs, TAG lenses can have much faster frame rates limited only by the liquid viscosity and sound speed. The frame rate of the example presented above was 1 kHz. If the voltage signal was not precisely periodic in time, but varied slightly with each repetition, then pattern variations could be achieved at this rate. This proceeding used only steady state modelling, however with fully transient modelling even higher frame rates would be possible. Compared to binary ferroelectric SLMs, TAG lenses allow for continuously spatially varying phase delays. Because of the simplicity and flexibility in the optical materials used in a TAG lens, it is possible to design one to withstand extremely large incident laser energies. Due to its analog nature, TAG lenses also avoid pixellation issues.

In addition to their advantages, TAG lenses do have some limitations that may make SLMs more suitable in certain applications. Specifically, TAG lenses work best when illuminated periodically with a small duty cycle, whereas SLMs are “always-on” devices. In some special cases, continuous wave illumination of TAG lenses may be acceptable if the index pattern in the middle of the cycle is not disruptive.

Despite the limitations of the TAG lens, in areas where fast switching and spatially continuous wavefront modulation are required, it should prove to be a valuable addition to the suite of available beam shaping devices as the technology progresses.

Acknowledgements

We wish to thank Clancy Rowley and Tracy Tsai for useful discussions, and Princeton University and AFOSR for financial support.

REFERENCES

1. M. P. MacDonald, G. C. Spalding, and K. Dholakia, "Microfluidic Sorting in an Optical Lattice," Nature **426**, 421–424 (2003).
2. K. Ladavac, K. Kasza, and D. G. Grier, "Sorting Mesoscopic Objects with Periodic Potential Landscapes: Optical Fractionation," Phys. Rev. E **70**, 010,901 (2004).
3. A. Terray, J. Oakey, and D. W. M. Marr, "Microfluidic Control Using Colloidal Devices," Science **296**, 1841–1844 (2002).
4. C. Bechinger, M. Brunner, and P. Leiderer, "Phase Behavior of Two-Dimensional Colloidal Systems in the Presence of Periodic Light Fields," Phys. Rev. Lett. **86**(5), 930–933 (2001).
5. K. Mangold, P. Leiderer, and C. Bechinger, "Phase Transitions of Colloidal Monolayers in Periodic Pinning Arrays," Phys. Rev. Lett. **90**(15), 158,302 (2003).
6. P. Korda, G. C. Spalding, E. R. Dufresne, and D. G. Grier, "Nanofabrication with Holographic Optical Tweezers," Rev. Sci. Instrum. **73**(4), 1956–1957 (2002).
7. J. Arlt and M. J. Padgett, "Generation of a Beam with a Dark Focus Surrounded by Regions of Higher Intensity: The Optical Bottle Beam," Opt. Lett. **25**(4), 191–193 (2000).
8. F. K. Fatemi and M. Bashkansky, "Cold Atom Guidance Using a Binary Spatial Light Modulator," Opt. Express **14**(4), 1368–1375 (2006).
9. J. E. Curtis, B. A. Koss, and D. G. Grier, "Dynamic Holographic Optical Tweezers," Opt. Commun. **207**, 169–175 (2002).
10. D. McGloin, G. C. Spalding, H. Melville, W. Sibbett, and K. Dholakia, "Applications of Spatial Light Modulators in Atom Optics," Opt. Express **11**(2), 158–166 (2003).
11. W. J. Hossack, E. Theofanidou, and J. Crain, "High-Speed Holographic Optical Tweezers Using a Ferroelectric Liquid Crystal Microdisplay," Opt. Express **11**(17), 2053–2059 (2003).
12. E. McLeod, A. B. Hopkins, and C. B. Arnold, "Multiscale Bessel Beams Generated by a Tunable Acoustic Gradient Index of Refraction Lens," Opt. Lett. **31**(21), 3155–3157 (2006).
13. T. Tsai, E. McLeod, and C. B. Arnold, "Generating Bessel Beams with a Tunable Acoustic Gradient Index of Refraction Lens," in *Proc. SPIE Vol. #6326* (SPIE, 2006). In press.
14. Euan McLeod and Craig B. Arnold. To be published.